Contracts Nonr 839(34) and Nonr 839(38)

THE INVISCID CHEMICAL NONEQUILIBRIUM FLOW BEHIND A MOVING NORMAL SHOCK WAVE

by

Dominic J. Palumbo and Ephraim L. Rubin

Distribution of this document is unlimited.

JUNE 1968

POLYTECHNIC INSTITUTE OF BROOKLYN

DEPARTMENT
of
AEROSPACE ENGINEERING
and
APPLIED MECHANICS

PIBAL REPORT NO. 68-18

THE INVISCID CHEMICAL NONEQUILIBRIUM FLOW BEHIND A MOVING NORMAL SHOCK WAVE

by

Dominic J. Palumbo and Ephraim L. Rubin

This research was conducted in part under Conract Nonr 839(34), and under Contract Nonr 839(38) for PROJECT DEFENDER, and was made possible by the support of the Advanced Research Projects Agency under Order No. 529 through the Office of Naval Research.

POLYTECHNIC INSTITUTE OF BROOKLYN

Department

of

Aerospace Engineering and Applied Mechanics

June 1968

PIBAL REPORT NO. 68-18

THE INVISCID CHEMICAL NONEQUILIBRIUM FLOW BEHIND A MOVING NORMAL SHOCK WAVE[†]

by

Dominic J. Falumbo[*] and Ephraim L. Rubin[**]

ABSTRACT

A time-dependent numerical scheme is used to solve for the chemical nonequilibrium profile behind a normal shock wave in air. The steady state equations are also integrated using a fourth order Runge-Kutta technique and a comparison is made with the time-dependent calculation. The results agree within one percent except in the region close to the shock. In this region the profiles differ because the time-dependent technique allows calculation through the shock (which is several mesh points in width) and as a result some dissociation occurs.

[†] This research was conducted in part under Contract Nonr 839(34), and under Contract Nonr 839(38) for PROJECT DEFENDER, and was made possible by the support of the Advanced Research Projects Agency under Order No. 529 through the Office of Naval Research. The authors would like to thank Prof. Stanley G. Rubin for a very helpful discussion.

[*] NDEA Trainee.

[**] Associate Professor of Aerospace Engineering.

TABLE OF CONTENTS

LIST OF ILLUSTRATIONS

I. INTRODUCTION

A good deal of effort has been devoted to studying gas dynamic problems, including the effects of chemical reactions. Earlier work generally involved systems with a single dissociation-recombination reaction. A survey of flow studies of that class has been given by Li [1]. More recent investigations have involved the study of gas dynamic flows with a series of coupled chemical reactions. The work of Marrone [2] is an example of calculations of this type. These results have all been obtained by solving the steady state equations.

In this paper we use a time dependent technique to solve for the nonequilibrium region behind a normal shock wave moving in air. We do not consider the discontinuities to be internal moving boundaries but rather obtain their motion from the solution of the differential equations. Hence the methods used to integrate the differential equations yield weak solutions in the space time domain.

As initial conditions for this problem, we choose a discontinuous function consisting of two constant equilibrium states. The fluid particles at equilibrium ahead of the shock move through the shock into the equilibrium state behind. The concentrations of the various species within the particle are no longer in equilibrium with the new temperature and pressure and chemical reactions begin to occur. Since the velocity of the fluid behind the shock is less than the shock velocity, the distance between the two original equilibrium states increases until sufficient time has elapsed to bring the entire system to a steady state, relative to the shock. The gas is assumed to be thermally perfect and in local thermodynamic equilibrium.

In a previous paper[3] one of us presented results for a calculation of this type for a Lighthill gas using a first-order scheme. In this paper we use a scheme which is more accurate and do the calculation for a six reaction model for air.

II. CHEMICAL MODEL

The i^{th} of r reactions involving species j may be written as

$$\sum_{j=1}^{s} a_{ij} M_j \underset{K_{b_i}}{\overset{K_{f_i}}{\rightleftharpoons}} \sum_{j=1}^{s} b_{ij} M_j \qquad (i = 1, \ldots . r)$$

where the a_{ij} and b_{ij} are the stoichiometric coefficients of species j, M_j is the chemical formula for species j and K_{f_i} and K_{b_i} are the forward and backward reaction rate constants for the i^{th} reaction.

The molar rate of production of species j due to reaction i is given by

$$\sigma_{ij} = (b_{ij} - a_{ij}) K_{f_i} \left[\prod_{\alpha=1}^{s} C_\alpha^{\,a_{i\alpha}} - \frac{1}{K_{c_i}} \prod_{\alpha=1}^{s} C_\alpha^{\,b_{i\alpha}} \right] \tag{1}$$

where K_{c_i} is the equilibrium constant based on molar concentrations and the C_α 's are the molar concentrations.

The total rate of production of species j is the sum of the rates of production of species j over all r reactions.

$$\sigma_j = \sum_{i=1}^{r} \sigma_{ij} \tag{2}$$

For each atom in the mixture there will be an equation of the form

$$\sum_{j=1}^{s} \sigma_j \mu_{ij} = 0 \tag{3}$$

where μ_{ij} is the number of atoms of the j^{th} element per molecule of the

i^{th} species. This relationship expresses the conservation of the j^{th} element and allows computation of the σ_j for elements in terms of the σ_j for molecules.

The following six reactions are the assumed chemical model for air:

$O_2+M \rightleftharpoons 2O+M$ (a)

$N_2+M \rightleftharpoons 2N+M$ (b)

$NO+M \rightleftharpoons N+O+M$ (c)

$NO+O \rightleftharpoons O_2+N$ (d)

$N_2+O \rightleftharpoons NO+N$ (e)

$N_2+O_2 \rightleftharpoons 2NO$ (f)

The species M in the first three reactions may be O_2, O, N_2, N, NO or Ar. In general, there is a different forward rate constant associated with each M. The forward rate and equilibrium constants used have the following form:

$$K_f=A_f T^{q_f} \exp\left(-\frac{E_{of}}{T}\right)$$

$$K_c=A_c T^{q_c} \exp\left(-\frac{E_{oc}}{T}\right)$$

Values for the constants A_f, A_c, q_f, q_c, E_{of}, and E_{o_c} are listed in Table I.

The first three reactions involve dissociation by two body collisions and lead to the formation of atoms by the direct dissociation of the molecules. The reverse reactions lead to molecular formation through atom recombination by three body collisions. Reactions (d), (e), and (f) are bimolecular exchange reactions.

III. DIFFERENTIAL EQUATIONS

The equations to be solved may be written in the following vector form:

$$w_t = f_x + S \tag{4}$$

where w is a vector function of x and t.

$$w = \begin{pmatrix} m \\ E \\ C_{O_2} \\ C_{N_2} \\ C_{NO} \\ C_N \\ C_O \\ C_{Ar} \end{pmatrix}$$

f is a given nonlinear function of w, i.e.,

$$f = -\begin{pmatrix} \frac{m^2}{\rho} + p \\ \frac{m}{\rho}(E + p) \\ \frac{m}{\rho} C_{O_2} \\ \frac{m}{\rho} C_{N_2} \\ \frac{m}{\rho} C_{NO} \\ \frac{m}{\rho} C_O \\ \frac{m}{\rho} C_N \\ \frac{m}{\rho} C_{Ar} \end{pmatrix}$$

and

$$S = \begin{pmatrix} 0 \\ 0 \\ \sigma_{O_2} \\ \sigma_{N_2} \\ \sigma_{NO} \\ \sigma_{O} \\ \sigma_{N} \\ \sigma_{Ar} \end{pmatrix}$$

The momentum m and total energy E are defined per unit volume. The total energy is the sum of the kinetic energy $\frac{m^2}{2\rho}$ and the internal energy ρe.

$$E = \rho e + \frac{m^2}{2\rho} \tag{5}$$

The total mass density ρ is given by:

$$\rho = \sum_{j=1}^{s} W_j C_j \tag{6}$$

where W_j is the molecular weight of species j.

For our equation of state we use

$$p = C_T R_o T \tag{7}$$

where

$$C_T = \sum_{j=1}^{s} C_j$$

Eqs. (4), (6), and (7) contain one more variable than number of equations. An additional relationship may be obtained from the definition of enthalpy, h.

$$h = e + \frac{p}{\rho}$$

Using Eqs. (5) and (7) yields

$$h - \frac{C_T R_o T}{\rho} - \frac{1}{\rho}\left(E - \frac{m^2}{2\rho}\right) = 0 \qquad (8)$$

The specific enthalpy of the mixture is given by

$$h = \frac{1}{\rho} \sum_{j=1}^{s} C_j H_j \qquad (9)$$

where we have introduced H_j for the molar enthalpy of species j. The data from Ref. 4 has been curve fitted using the method of least squares to obtain a quadratic expression for the molar enthalpy.

$$H_j = A_j T^2 + B_j T + H^o_{f_j} \qquad (10)$$

where $H^o_{f_j}$ is the molar heat of formation of species j at 0^oK. Values of A_j, B_j and $H^o_{f_j}$ used are listed in Table II. Substitution of Eqs. (9) and (10) into Eq. (8) yields the following expression for the temperature:

$$T = \frac{D_1}{2A}\left[\sqrt{1 + \frac{4AD_2}{D_1^2}} - 1\right] \qquad (11)$$

where

$$D_1 = \sum_{j=1}^{s} C_j (B_j - R_o)$$

$$D_2 = E - \frac{m^2}{2\rho} - \sum_{j=1}^{s} C_j H^{o}_{f_j}$$

$$A = \sum_{j=1}^{s} C_j A_j$$

A specification of m, E and the C_j allows determination of ρ from Eq. (6), T from Eq. (11), and p from Eq. (7). Hence we have a closed system.

IV. INITIAL CONDITIONS AND DIFFERENCE SCHEMES

The initial condition consists of a uniformly moving discontinuity separating two equilibrium states. The upstream equilibrium state and propagation velocity of the discontinuity are specified. The Rankine-Hugoniot relationships are then used to obtain the corresponding downstream state:

$$\rho_1 u_1 = \rho_2 u_2 \tag{12}$$

$$p_1 + \rho_1 u_1^2 = p_2 + \rho_2 u_2^2 \tag{13}$$

$$h_1 + \tfrac{1}{2} u_1^2 = h_2 + \tfrac{1}{2} u_2^2 \tag{14}$$

In the above equations let subscripts 1 and 2 indicate the upstream and downstream states respectively. u_1 and u_2 are the velocities relative to the discontinuity. Several iterations are required to obtain state 2. Using Eqs. (12) and (13) we may write

$$\frac{\rho_1}{\rho_2} = 1 + \frac{1}{\gamma_1 M_1^2} \left(1 - \frac{p_2}{p_1} \right) \tag{15}$$

where γ is the ratio of the specific heat at constant pressure to the specific heat at constant volume and

$$M_1 = \frac{\rho_1 u_1^2}{\gamma_1 p_1}$$

is the relative upstream Mach number.

From the Eq. of state (7) we obtain

$$\frac{T_2}{T_1} = \frac{p_2}{p_1} \; \frac{\rho_1}{\rho_2} \; \frac{\overline{W}_2}{\overline{W}_1} \tag{16}$$

where

$$\overline{W} = \frac{1}{C_T} \sum_{i=1}^{s} C_i W_i$$

For the first step of the iteration procedure choose a value of p_2/p_1 and calculate ρ_2/ρ_1 from (15). Solve for T_2/T_1 using equation (16) with the assumption $\overline{W}_2 = \overline{W}_1$. With the values of T_2 and p_2 thus obtained, calculate the corresponding equilibrium composition. Since there are five possible products being considered as a result of chemical reaction between O_2 and N_2 there will be five unknown quantities; namely, the resulting concentration of each species. The five equations used to obtain these unknowns are the two atom conservation equations for oxygen and nitrogen and the three equations relating the equilibrium constants for the stoichiometric dissociation of O_2 and N_2 and formation of NO to the concentrations of each species.

Using the calculated concentrations obtain a new value of $\overline{W}_2$.

From equation (16) obtain a new value of T_2. Repitition of this iteration will yield a T_2, p_2, ρ_2 and composition satisfying equations (15) and (16). To determine whether T_2 satisfies the energy equation (14), write

$$h_2 = h_1 + u_1^2\left[1 - \left(\frac{\rho 1}{\rho 2}\right)^2\right]$$

h_1 is calculated from equation (9) and hence h_2 is known. We may also write h_2 as

$$h_2 = \frac{1}{\rho_2} \sum_{i=1}^{s} (C_i)_2 (H_i)_2$$

which, after substituting equation (10) for H_i yields

$$h_2 = \frac{1}{\rho_2}\left[\sum_{i=1}^{s} (C_i)_2 A_i T_2^2 + \sum_{i=1}^{s} (C_i)_2 B_i T_2 + \sum_{i=1}^{s} (C_i)_2 H^o_{f_i}\right] \qquad (17)$$

This equation is solved for T_2. If T_2 from equation (17) is not equal to the one found previously assume a new value of p_2/p_1 and repeat the procedure.

The initial value for p_2/p_1 is calculated assuming frozen flow and fixed γ. This value is then increased until the above conditions are met.

Time-dependent difference methods that may be used for the solution of equations (4) have been discussed by one of us in Ref. 5 . The two-step method used in this calculation is given below. In the first step a first order scheme is used to compute the intermediate values at twice t + Δt. We denote these intermediate values by a bar. A second order accurate scheme is used to compute the final values. The overall scheme has second order accuracy. The second step averages the f differences at t and t+Δt so that values of w, f, and S are all centered at the point $(n, t + \frac{\Delta t}{2})$.

$$\bar{w}^{t+\Delta t}_{n\pm\frac{1}{2}} = \frac{1}{2}(w^t_{n\pm1} + w^t_n) \pm \lambda(f^t_{n\pm1} - f^t_n) + \frac{\Delta t}{2}(S^t_n + S^t_{n\pm1})$$

$$\bar{\bar{w}}^{t+\Delta t}_n = \frac{1}{2}(w^t_{n+1} + w^t_{n-1}) + \frac{\lambda}{2}(f^t_{n+1} - f^t_{n-1}) + \frac{\Delta t}{2}(S^t_{n+1} + S^t_{n-1})$$

The bars signify intermediate values.

The final values are computed using

$$w_n^{t+\Delta t} = w_n^t + \frac{\lambda}{2}\left[\tfrac{1}{2}\left(f_{n+1}^t - f_{n-1}^t\right) + \overline{f}_{n+\frac{1}{2}}^{t+\Delta t} - \overline{f}_{n-\frac{1}{2}}^{t+\Delta t}\right] + \frac{\Delta t}{2}\left(S_n^t + \overline{S}_n^{t+\Delta t}\right) \tag{18}$$

where

$$\lambda = \frac{\Delta t}{\Delta x}$$

The initial conditions given below are for $M_1 = 10.03$ with upstream conditions representative of 150,000 feet above sea level.

ρ_2/ρ_1 = 9.67

p_2/p_1 = 126.75

T_2/T_1 = 11.91

X_{O_2} = 7.2169×10^{-2}

X_O = 1.9291×10^{-1}

X_{N_2} = 6.8441×10^{-1}

X_N = 1.7476×10^{-4}

X_{NO} = 4.2199×10^{-2}

X_{Ar} = 8.1311×10^{-3}

The X_i are the mole fractions, i.e., number of moles of species i per mole of mixture.

$$X_i = \frac{C_i}{C_T}$$

Since the initial conditions are equilibrium states all dependent variables remained constant ahead of the shock and in the region behind the relaxation zone.

It is well-known [5, 6] that the finite difference solution to Equations (4), with S = 0, for numerical schemes of the type employed here have an overshoot in flow variables immediately behind the shock. Inclusion of chemical reactions does not eliminate this overshoot since their effect is negligible through the shock. The overshoot in pressure, in particular, yields a value which exceeds that in the equilibrium region downstream. A fluid particle experiencing this numerical overshoot will relax along a different thermodynamic path and hence yield a different nonequilibrium profile. We chose to eliminate the overshoot by using a first order [7] scheme in the region close to the shock. The additional numerical viscosity of this scheme smooths out the overshoot but lowers the accuracy of the calculation in this region. The entire nonequilibrium region extends over two-hundred mesh points. The first order scheme is used at ten.

V. DISCUSSION OF RESULTS

Results presented in figures I through VIII correspond to a Mach number of 10.03 and upstream conditions representative of 150,000 feet above sea level. The calculation was performed using a time step of 1.175×10^{-6} seconds and results are plotted at time step six-hundred. Comparison with time step five-hundred indicated no change in the profile. Hence, these results are for a steady state relative to the shock. To check convergence a run was made for twice the number of time steps using half the value of Δt. Results were the same to within one percent. A further check on the solution was afforded using a fourth order Runge-Kutta scheme to integrate the steady state equations. Jump conditions based on frozen composition were used as the initial condition for this calculation. Comparison between the steady-state and time-dependent techniques showed the to be in agreement to within a percent except in a region close to the shock. The results differ in this region because the time-dependent technique allows calculation through the shock (which is several mesh points in width) and as a result some dissociation occurs. Thus, the jump conditions obtained are not based on frozen composition. The jump conditions based on frozen composition and those obtained using the time-dependent method are listed below for comparison.

		Frozen	Calculated
p_2/p_1	=	121.0892	119.7179
T_2/T_1	=	17.3466	16.3469
ρ_2/ρ_1	=	6.9806	7.1774
X_{O_2}	=	.21	.174726
X_O	=	0	.039803
X_{N_2}	=	.781	.754165
X_N	=	0	.000126
X_{NO}	=	0	.022359
X_{Ar}	=	.009	.008821

Figure 1 shows the effect of the chemical system on the temperature. Immediately behind the shock the temperature is 4500°K. It then decreases monotonically through the relaxation region to its equilibrium value of about 3300°K. The total density increases about 30% from its value immediately behind the shock (Figure 2) whereas the pressure remains practically constant after a slight initial rise (Figure 3).

Figure 4 shows the decrease in mole fraction of O_2 as the distance from the shock increases and Figure 5 shows the corresponding formation of the atomic species O. The molecular species N_2 decreases monotonically behind the shock (Figure 6) but N and NO have maxima (Figures 7 and 8).

The NO maximum has been observed experimentally [8]. The reason for the maximum in the NO and N mole fraction follows from an analysis of the reaction rates through the nonequilibrium region. Because of the initial abundance of 0_2 and N_2 reaction (f) is at first a major produces of NO. Since reaction (a) is relatively fast 0_2 decomposes into 0 atoms quickly. As 0 appears reaction (e) begins production of NO and N. Reaction (d) initially proceeds to the left making this reaction a major contributor to the amount of NO. Farther downstream of the shock reactions (e) and (f) reverse and proceed to the left until equilibrium is obtained. Reaction (d) also reverses and proceeds to the right as equilibrium is approached. When this occurs NO and N begin to diminish. Hence we get maxima in their mole fractions at approximately the same point behind the shock.

For inviscid flows with chemistry the Runge-Kutta integration of the steady state equations is faster and slightly more accurate. The advantage of the time-dependent method lies in its ease of extension to viscous, heat conducting, and radiating flows. With dissipative effects there is no numerical overshoot and the calculation may be done without the introduction of the lower order scheme in the region of the shock. We hope to report soon on a calculation of this type.

VI. REFERENCES

1. Li, T. Y., "Recent Advances in Nonequilibrium Dissociating Gasdynamics", ARS Journal, February 1961.
2. Marrone, P. V., "Inviscid Nonequilibrium Flow Behind Bow and Normal Shock Waves", Report No. QM-1626-A-12, 1963, Cornell Aeronautical Laboratory, Inc., Buffalo, N.Y.
3. Bohachevsky, I. O. and Rubin, E. L., "A Direct Method for Computation of Nonequilibrium Flows with Detached Shock Waves", AIAA Journal, Vol. 4, No. 4, April 1966, pp. 600-607.
4. "Thermodynamic Properties to 6000°K for 210 Substances Involving the First 18 Elements", NASA SP-3001, 1963.
5. Rubin, E. L. and Burstein, S. Z., "Difference Methods for the Inviscid and Viscous Equations of a Compressible Gas", Journal of Computational Physics, Vol. 2, No. 2, November 1967, pp. 178-196.
6. Lax, P. and Wendroff, B., "Systems of Conservation Laws", Communications on Pure and Applied Mathematics, Vol. 13, 1960, pp. 217-237.
7. Lax, P. D., "Weak Solutions of Nonlinear Hyperbolic Equations and Their Numerical Computation", Communications on Pure and Applied Mathematics, Vol. 7, 1954, pp. 159-193.
8. Allport, J. J., "Formation of Nitric Oxide Behind Strong Shock Waves in Air", Report LMSD-288226, Jan. 1960, Lockheed Aircraft Corp.

TABLE I

FORWARD RATE AND EQUILIBRIUM CONSTANTS

Reaction	Catalytic Body	A_f	q_f	E_{of}(^{o}K)	A_c	q_c	E_{oc} (^{o}K)
(a)	Ar, NO, N	3.6 (19)	-1.0	5.95 (4)	1.2 (3)	-0.5	5.95 (4)
	N_2	4.8 (20)	-1.5	5.95 (4)	1.2 (3)	-0.5	5.95 (4)
	O_2	1.9 (21)	-1.5	5.95 (4)	1.2 (3)	-0.5	5.95 (4)
	O	6.4 (23)	-2.0	5.95 (4)	1.2 (3)	-0.5	5.95 (4)
(b)	Ar, O_2, NO, O	1.9 (17)	-0.5	1.13 (5)	18.0	0.0	1.13 (5)
	N_2	4.8 (17)	-0.5	1.13 (5)	18.0	0.0	1.13 (5)
	N	4.1 (22)	-1.5	1.13 (5)	18.0	0.0	1.13 (5)
(c)	Ar, N_2, O_2	3.9 (20)	-1.5	7.55 (4)	4.0	0.0	7.55 (4)
	NO, O, N	7.9 (21)	-1.5	7.55 (4)	4.0	0.0	7.55 (4)
(d)	----	3.2 (9)	+1.0	1.97 (4)	3.3 (-3)	+0.5	1.60 (4)
(e)	----	7.0 (13)	0.0	3.80 (4)	4.5	0.0	3.75 (4)
(f)	----	4.6 (24)	-2.5	6.46 (4)	1.35 (3)	-0.5	2.15 (4)

Note: (N) = 10^N

TABLE II

COEFFICIENT FOR ENTHALPY CURVE FIT

Species	A_i (erg/mole/$^oK^2$)	B_i (erg/mole/^oK)	$H^o_{f_i}$ (erg/mole)
O_2	7.3947250136(+3)	3.2540448331(+8)	0
O	2.4291027537(+2)	2.1092339308(+8)	2.4677232(+12)
N_2	8.2344462242(+3)	3.1075207522(+8)	0
N	2.5865494701(+3)	2.0048830691(+8)	4.7078368(+12)
NO	7.8127087774(+3)	3.1875545777(+8)	0.8985977(+12)
Ar	0	2.0786725000(+8)	0

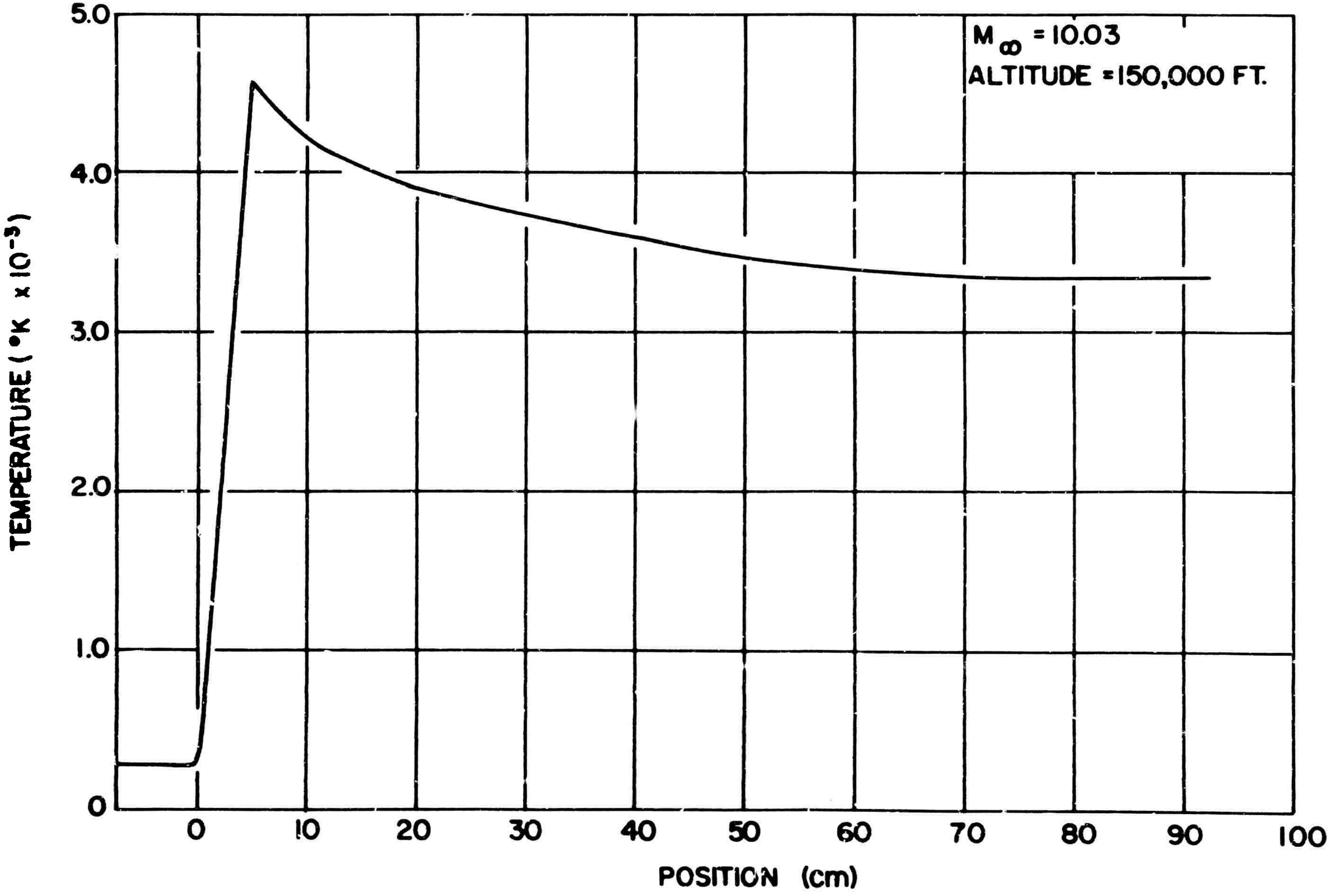

FIG. 1 TEMPERATURE VS POSITION

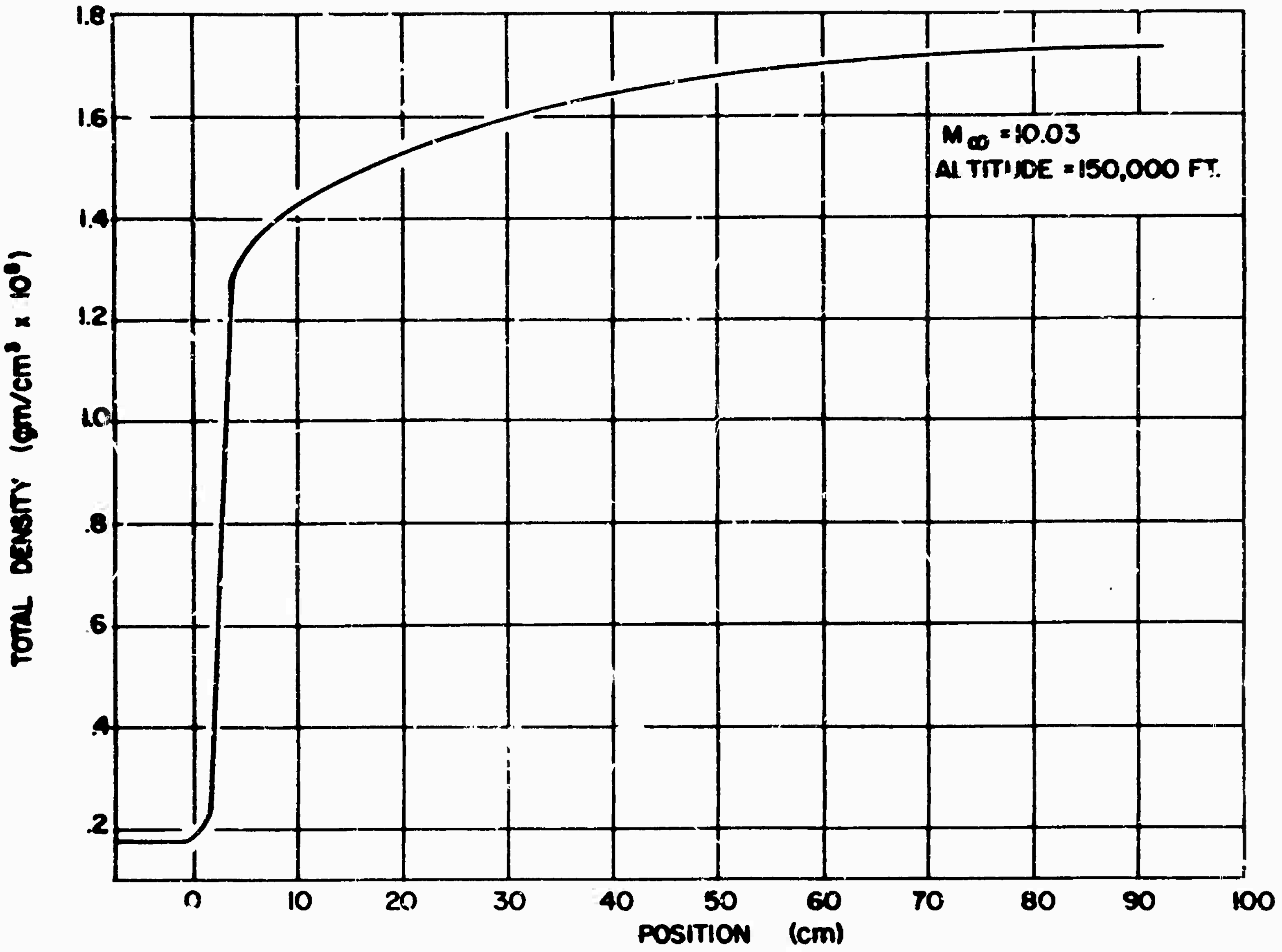

FIG. 2 TOTAL DENSITY VS. POSITION

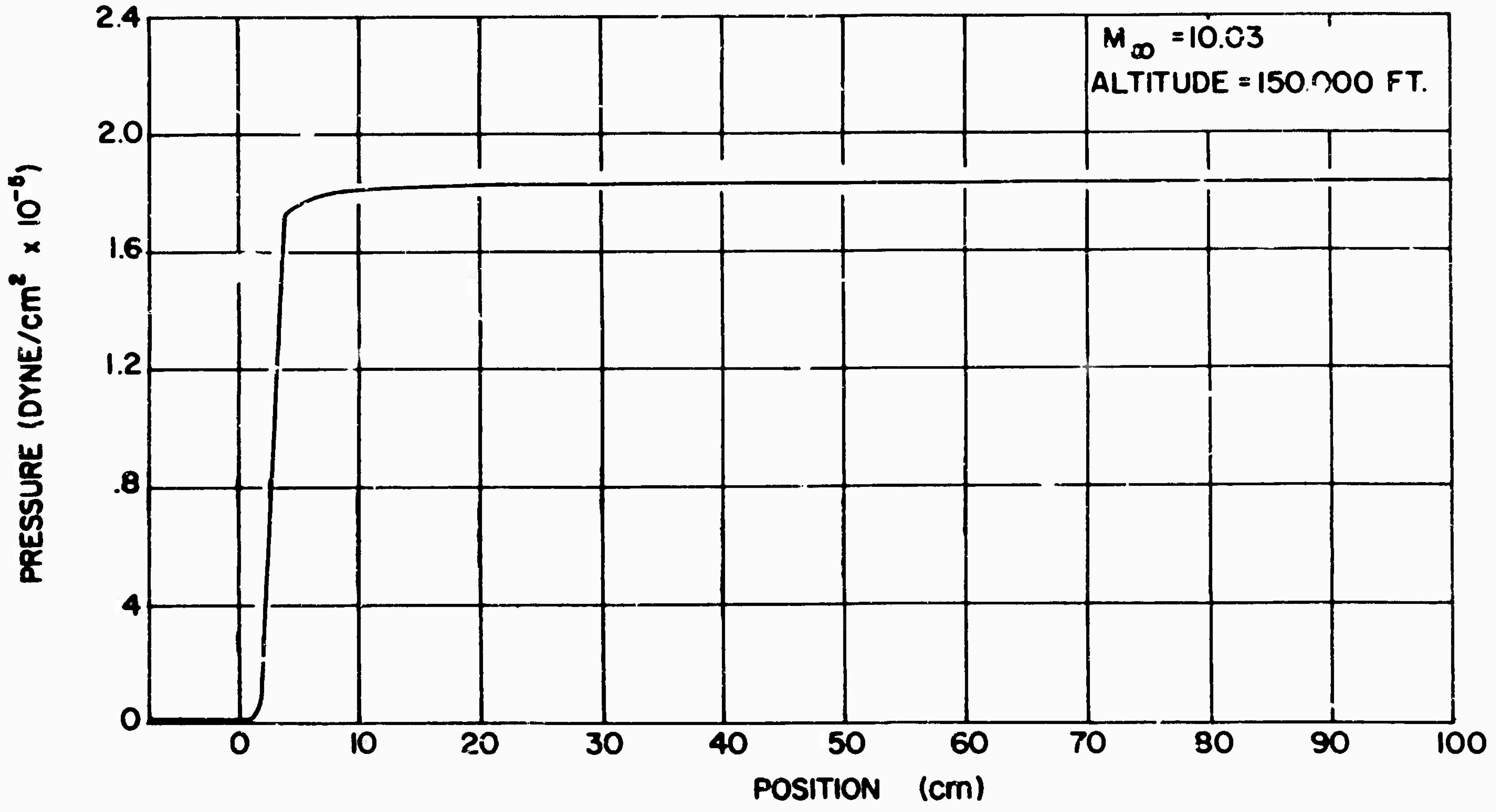

FIG. 3 PRESSURE VS. POSITION

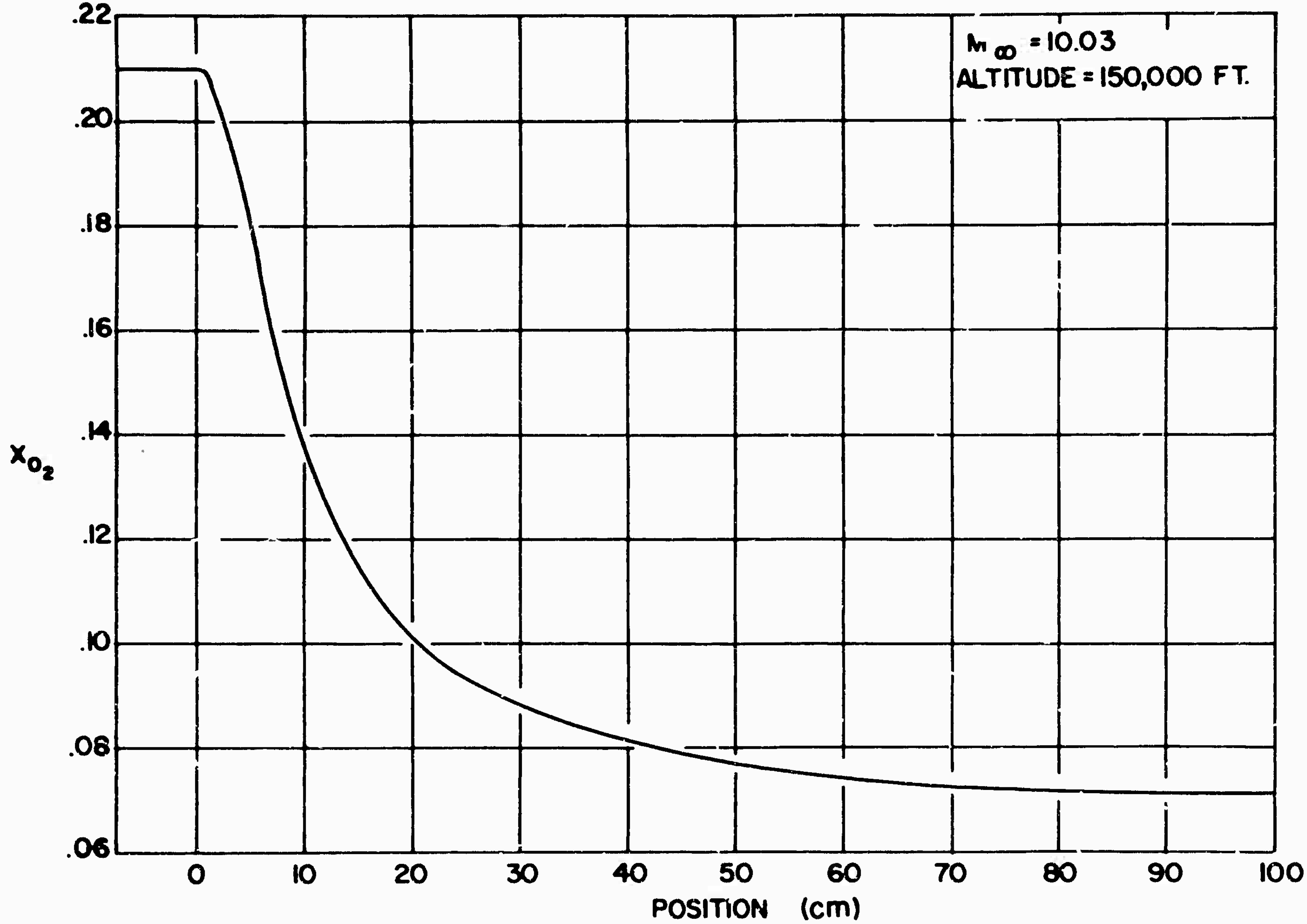

FIG. 4 MOLE FRACTION O_2 VS. POSITION

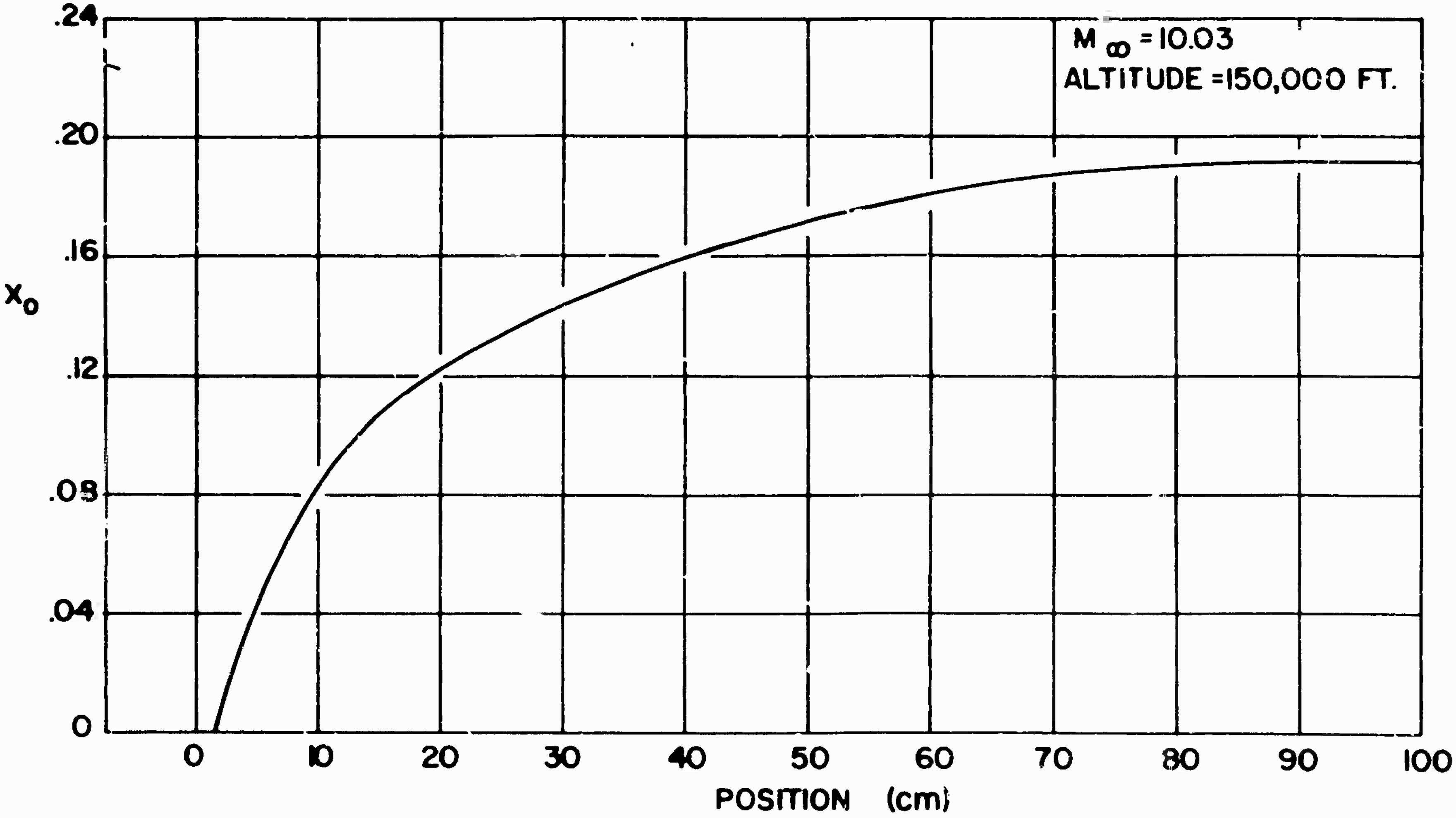

FIG. 5 MOLE FRACTION O VS. POSITION

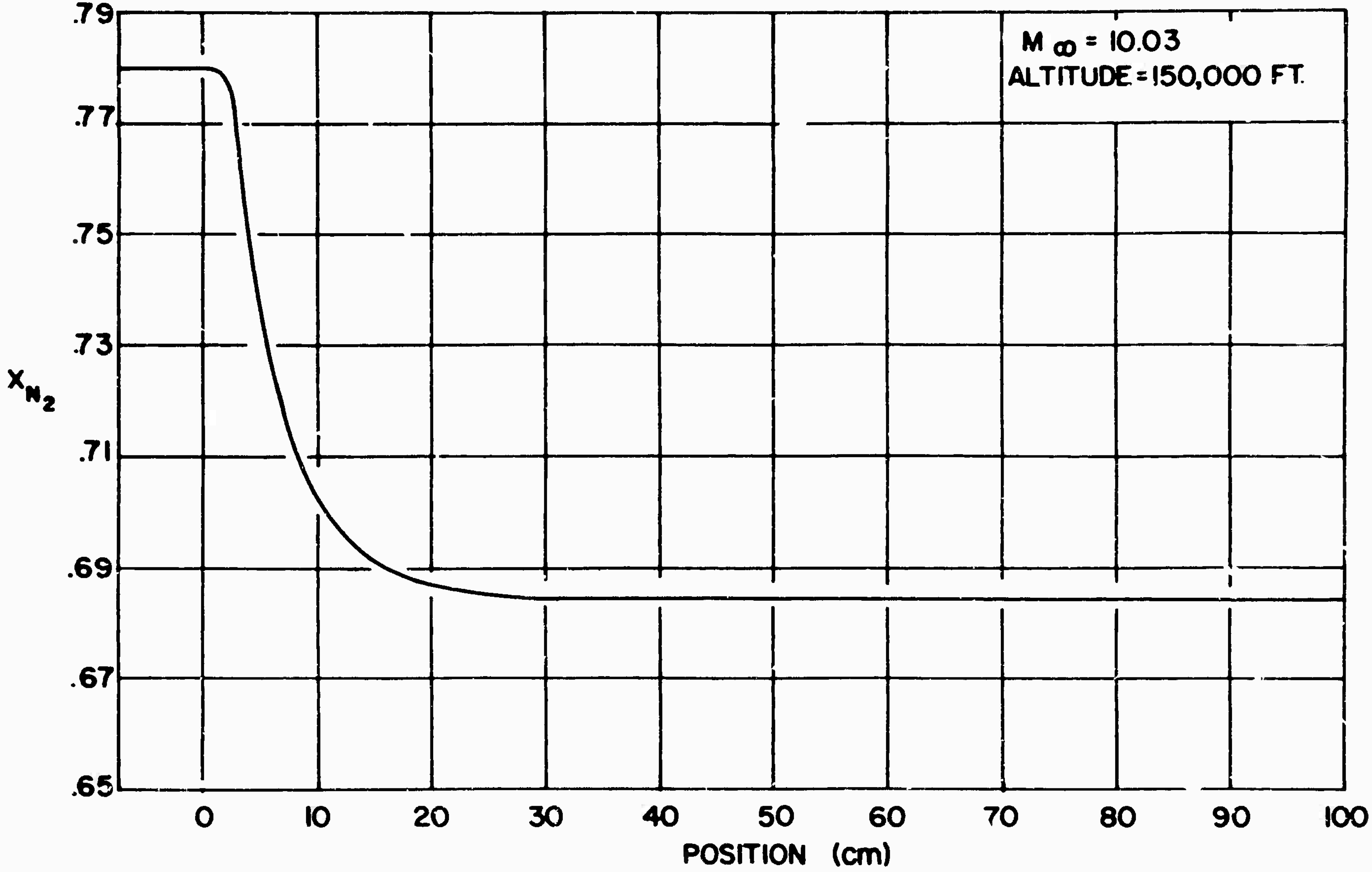

FIG. 6 MOLE FRACTION N_2 VS. POSITION

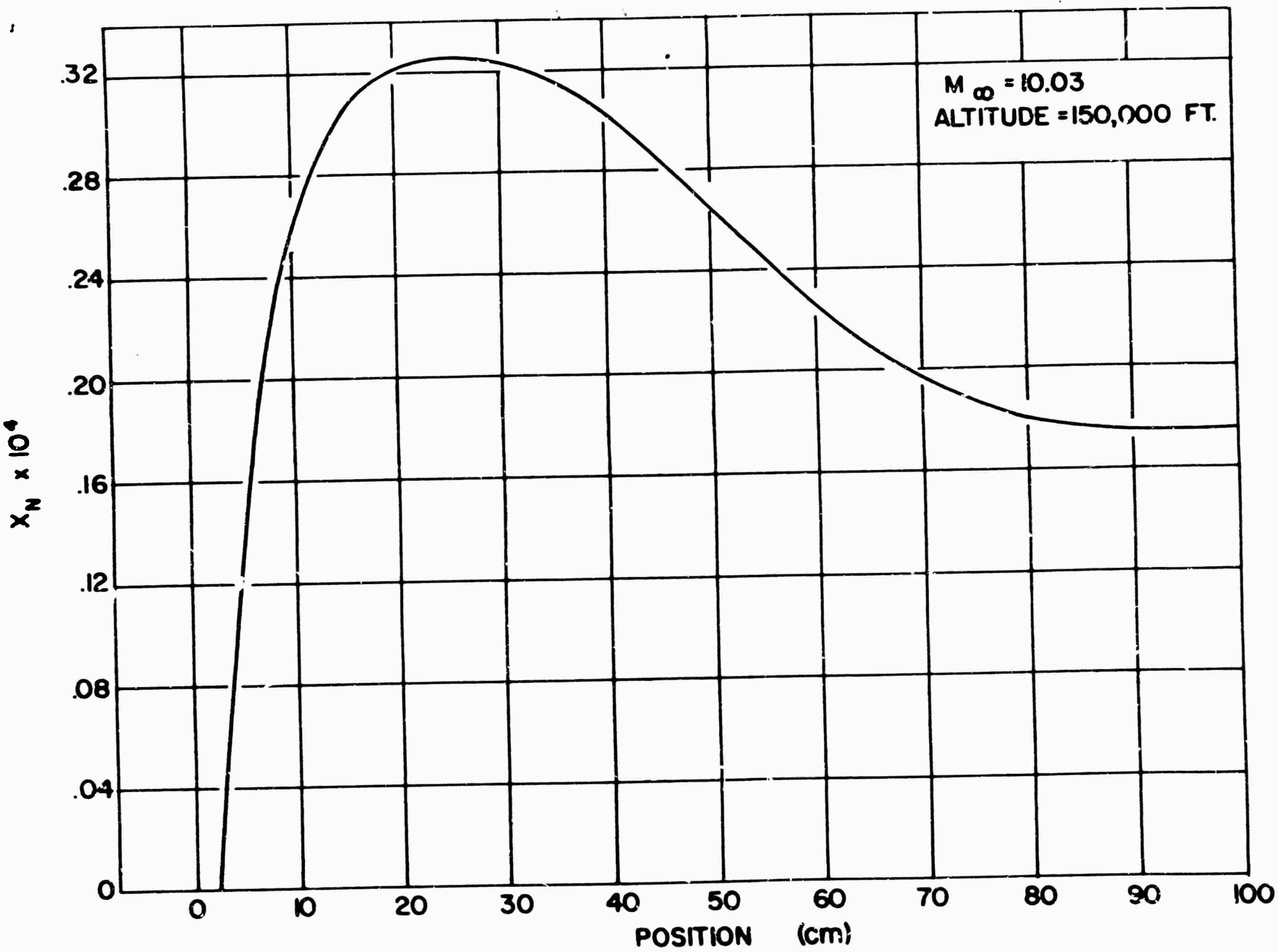

FIG. 7 MOLE FRACTION N VS. POSITION

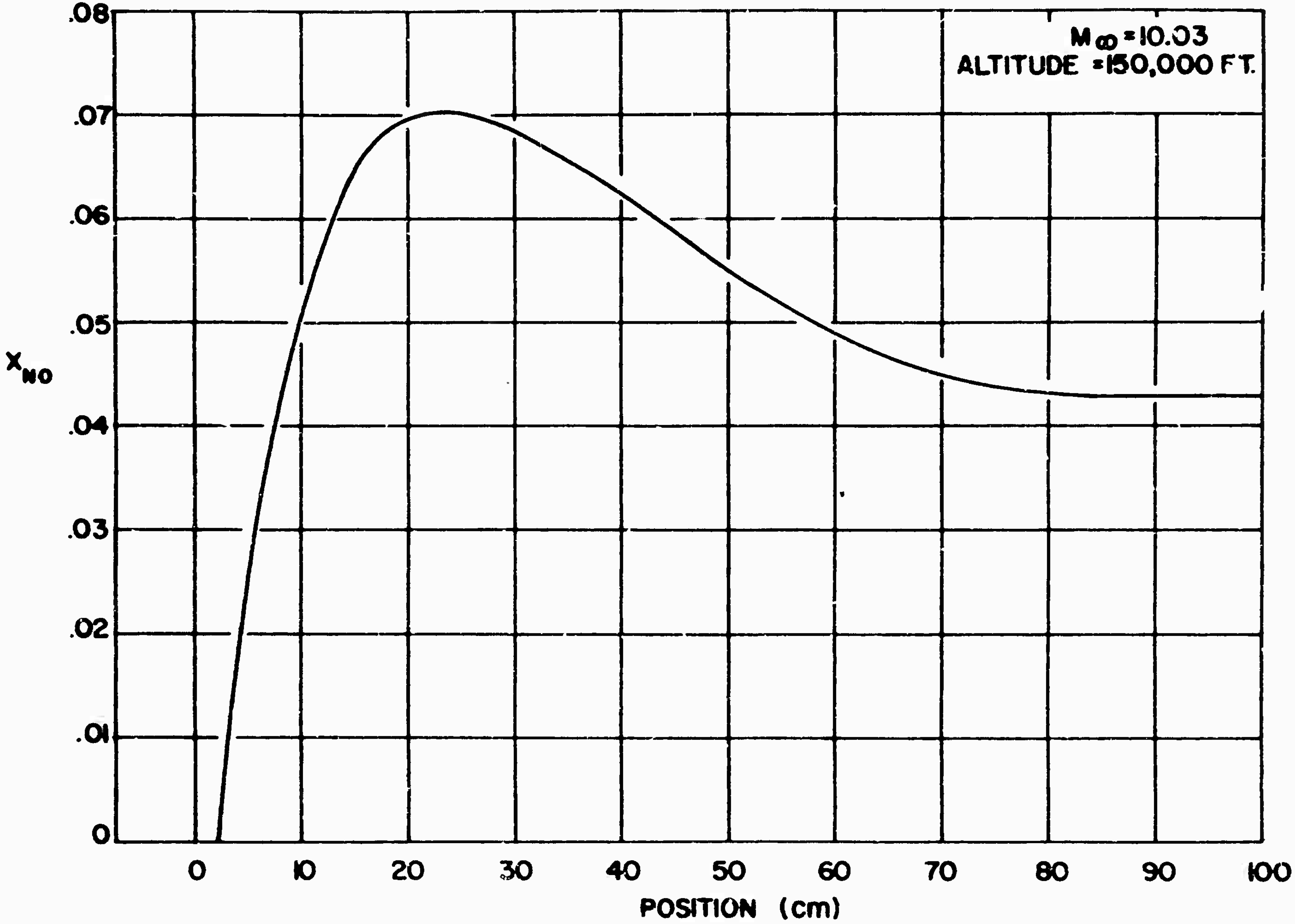

FIG. 8 MOLE FRACTION NO VS. POSITION

DOCUMENT CONTROL DATA - R & D

(Security classification of title, body of abstract and indexing annotation must be entered when the overall report is classified)

1. ORIGINATING ACTIVITY *(Corporate author)* Polytechnic Institute of Brooklyn Graduate Center Dept. of Aerospace Engineering & Applied Mechanics Route 110, Farmingdale, New York 11735	2a. REPORT SECURITY CLASSIFICATION Unclassified 2b. GROUP

3. REPORT TITLE

THE INVISCID CHEMICAL NONEQUILIBRIUM FLOW BEHIND A MOVING NORMAL SHOCK WAVE

4. DESCRIPTIVE NOTES *(Type of report and inclusive dates)*

Research Report

5. AUTHOR(S) *(First name, middle initial, last name)*

Dominic J. Palumbo and Ephraim L. Rubin

6. REPORT DATE June 1968	7a. TOTAL NO. OF PAGES 24	7b. NO. OF REFS 8

8a. CONTRACT OR GRANT NO. Nonr 839(34) and Nonr 839(38) b. PROJECT NO. NR 061-135 c. ARPA Order No. 529 d.	9a. ORIGINATOR'S REPORT NUMBER(S) PIBAL REPORT NO. 68-18 9b. OTHER REPORT NO(S) *(Any other numbers that may be assigned this report)*

10. DISTRIBUTION STATEMENT

Distribution of this document is unlimited.

11. SUPPLEMENTARY NOTES	12. SPONSORING MILITARY ACTIVITY Office of Naval Research Department of the Navy Washington, D.C. 20360

13. ABSTRACT

A time-dependent numerical scheme is used to solve for the chemical nonequilibrium profile behind a normal shock wave in air. The steady state equations are also integrated using a fourth order Runge-Kutta technique and a comparison is made with the time-dependent calculation. The results agree within one percent except in the region close to the shock. In this region the profiles differ because the time-dependent technique allows calculation through the shock (which is several mesh points in width) and as a result some dissociation occurs.

14. KEY WORDS	LINK A		LINK B		LINK C	
	ROLE	WT	ROLE	WT	ROLE	WT
Fluid Dynamics						
Chemistry						
Steady State						
Time-Dependent						